Multi-focus Image Fusion Using Spatial Frequency and Genetic Algorithm

Jun Kong[†, ††], **Kaiyuan Zheng**[†, †††], **Jingbo Zhang**[†, ††,*], **Xue Feng**[†, ††]

[†]Computer school, Northeast Normal University, Changchun, China
[††] Key Laboratory for Applied Statistics of MOE, China
[†††] College of Humanities and Sciences of Northeast Normal University, Changchun, China

Summary
We introduce in this paper a region based multi-focus image fusion algorithm using spatial frequency and genetic algorithm. The basic idea is to divide the source images into blocks, and then select the corresponding blocks with higher spatial frequency value to construct the resultant fused image. GA is brought forward to determine the suitable sizes of the block.

Key words:
Multi-focus image fusion, genetic algorithm, spatial frequency.

1. Introduction

A wide variety of data acquisition devices are available at present, and hence image fusion has become an important There are a number of techniques for multi-focus image fusion. Simple techniques in which the fusion operation is performed directly on the source images (e.g. weighted average method), often have serious side effects like reduction in the contrast of the fused image. Other approaches include, image fusion using controllable camera [2], probabilistic methods [3], image gradient method with majority filtering [4], multi-scale methods [5] and multi-resolution approaches [6]–[9]. Methods described in [2] depend on controlled camera motion and do not work for arbitrary set of images. Probabilistic techniques involve huge computation using floating point arithmetic and thus require a lot of time and memory-space. Image gradient method with majority filtering has the drawback that the defocused zone of one image is enhanced at the expense of focused zone of others.

We introduce in this paper a region based multi-focus image fusion algorithm using spatial frequency and genetic algorithm (GA), which combines pixel-level and feature-level fusion. The basic idea is to divide the source images into blocks, and then select the corresponding blocks with higher spatial frequency value to construct the resultant fused image. GA is brought forward to determine the suitable sizes of the block. The advantages of our method are the simplicity of computation and the automation of selecting the block sizes. And the resultant fused images are both qualitatively and visually superior to those produced by the Haar wavelet method and morphological wavelet approach, particularly when there is movement in the objects or mis-registration of the source images.

The rest of this paper is organized as follows. Section 2 gives the brief introduction of the spatial frequency. Section 2 introduction of the GA The proposed fusion scheme is described in Section4. Experimental results and discussion are presented in Section 5.

2. Spatial Frequency

Spatial frequency [10] measures the overall activity level in an image. For an $M \times N$ image block F, with gray value $F(m,n)$ at position (m,n), the spatial frequency is defined as

$$SF = \sqrt{RF^2 + CF^2} \quad (1)$$

Where RF and CF are the row frequency

$$RF = \sqrt{\frac{1}{MN}\sum_{m=1}^{M}\sum_{n=2}^{N}[F(m,n) - F(m,n-1)]^2} \quad (2)$$

And column frequency

$$CF = \sqrt{\frac{1}{MN}\sum_{n=1}^{N}\sum_{m=2}^{M}[F(m,n) - F(m-1,n)]^2} \quad (3)$$

Fig.1 (a) shows a 256×256 image block extracted from the 'Lab' image. Fig.1 (b)-(d) show the degraded versions after blurring with a Gaussian of radius 0.5, 1, 2, respectively. It can be seen from TABLE 1 that when the image becomes more blurred, the spatial frequency value diminishes accordingly. This demonstrates that the spatial frequency can be used to reflect the clarity of an image.

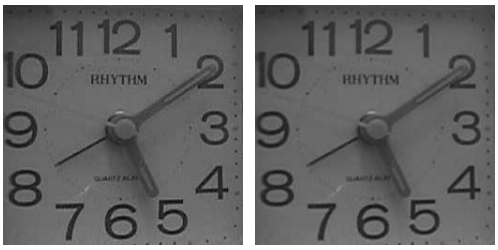

(a) (b)

* Corresponding author
This work is support by Science Foundation for Young Teachers of Northeast Normal University, NO. 20070603, and Training Fund of NENU'S Scientific Innovation Project, No. NENU-STC07018, China.

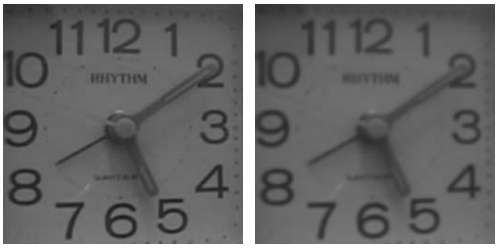

(c) (d)

Fig.1. Original and blurred versions of an image block from the 'Lab' image. (a) original image; (b) radius=0.5; (c) radius=1; (d) radius=2.

Table 1. Spatial Frequencies of the image block in Fig.1

	Fig.1(a)	***Fig.1(b)***	***Fig.1(c)***	***Fig.1(d)***
SF	11.6991	9.0366	7.0884	4.4917

3.Fundamental concepts of genetic algorithm

Assuming that we employ GA to search for the largest fitness value with a given fitness function. In GA, as shown in Fig. 2, the core components are depicted as follows [11][12].

(1) Select mate: A large portion of the low fitness individuals is discarded through this natural selection step. Of the N individuals in one iteration, only the top N_{good} individuals survive for mating, and the bottom $N_{bad} = N - N_{good}$ ones are discarded to make room for the new of springs in the next iteration. Therefore, the selection rate is N_{good} / N.

(2) Crossover: Crossover is the first way that a GA explores a fitness surface. Two individuals are chosen from N_{good} individuals to produce two new offspring. A crossover point is selected between the first and the last chromosomes of each individual after the crossover point are exchanged, and two new offspring are produced.

(3) Mutate: Mutation is the second way that a GA explores a fitness surface. It introduces traits not in the original individuals, and keeps GA from converging too fast. The pre-determined mutation rate should be low. Most mutations deteriorate the fitness of an individual, however, the occasional improvement of the fitness adds diversity and strengthens the individual. After obtaining the fundamental concepts in GA, we are able to design an optimized fusion system with the aid of GA.

4. Multi-focus image fusion

The problem to be solved here is as follows: Given two (or more) images of a stationary camera, it is required to combine the images into a single one that has all objects in focus without producing details that are non-existent in the given images. Although the fusion algorithm can be extended straightforwardly to handle more than two source images, we only consider the fusing of two source images for simplicity. The algorithm consists of the following steps:

(1) Decompose the source images A and B into blocks of size $M \times N$. Denote the *i*th blocks of A and B by A_i and B_i, respectively.

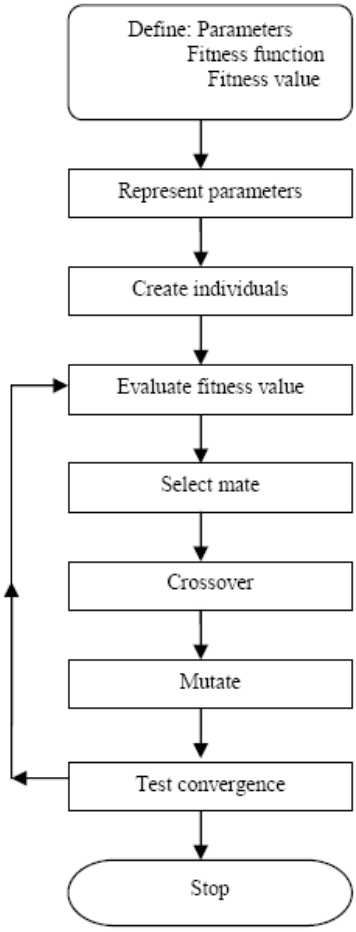

Fig. 2. The flow chart of genetic algorithm.

(2) Compute the spatial frequency of each block, and denote the spatial frequencies of A_i and B_i by SF_i^A and SF_i^B, respectively.

(3) Compare the spatial frequencies of two corresponding blocks A_i and B_i, and construct the *i*th block F_i of the fused image as

$$F_i = \begin{cases} A_i, & SF_i^A > SF_i^B + th, \\ B_i, & SF_i^A < SF_i^B - th, \\ \dfrac{A_i + B_i}{2}, & \text{otherwise} \end{cases} \quad (4)$$

Here, *th* is a user-defined threshold.

(4) Verify and correct the fusion result in step (3): specifically, if the center block comes from A, while the majority of its surrounding blocks are from B, then this center block will be changed to be from B, and vice versa. In the implementation, we use a majority filter together with a 3×3 window.

(5) Since different sizes of block can lead to different quality of resultant images, GA is employed to search for the optimized sizes of block.

5.Experimental results and discussion

We have compared our results with those obtained using Haar wavelet transform fusion and morphological wavelet fusion proposed by Ishita De and Bhabatosh Chanda [1]. The experimental results are shown in Fig. 3 and Fig. 4. In each figure, the reference image (all in focus) and source multi-focus images are given first, followed by resultant fused images produced by Haar wavelet, morphological wavelet and our proposed method. A clearer comparison can be made by examing the differences between the reference image and resultant image. The Haar wavelet transform and morphological wavelet are decomposed up to the third level.

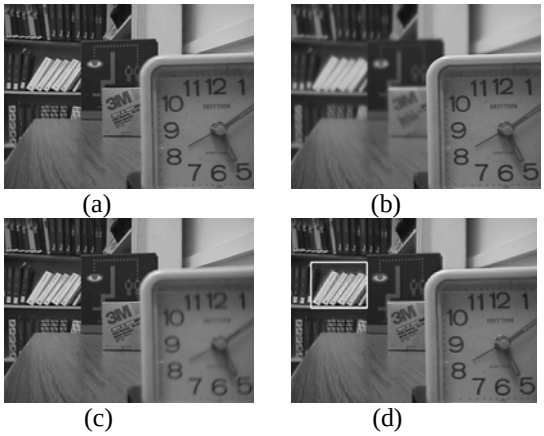

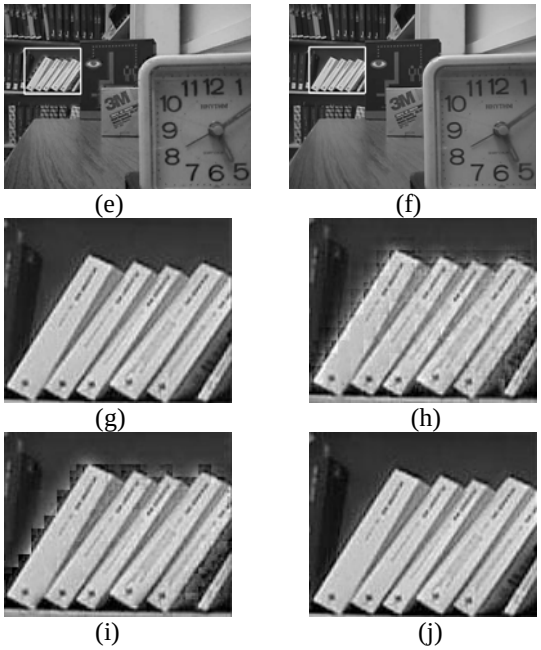

Fig. 3 The 'Disk' source images (size = 640 × 480) and fusion results: (a) reference image. (b) focus on the right. (c) focus on the left. (d) Haar wavelet result. (e) morphological wavelet result. (f) the result of the proposed algorithm. (g) - (j) are the local magnifications of (a), (d), (e) and (f), respectively.

A..Performance Analysis

Careful inspection of Fig. 3 and Fig. 4 reveals that the results obtained by the proposed method are better than that of Haar wavelet transform method and morphological wavelet method, particularly when there is a slight movement of the student's head in Fig. 4 (b) and (c). However, this is a subjective measure of quality and may not be universally acceptable. Hence root mean squared error (RMSE) measure and similarity measure [1] are also adopted.

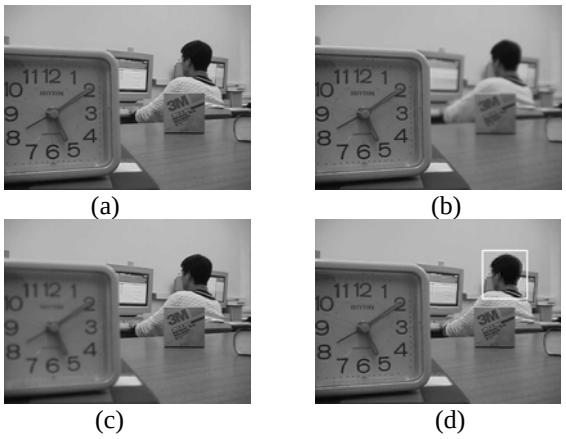

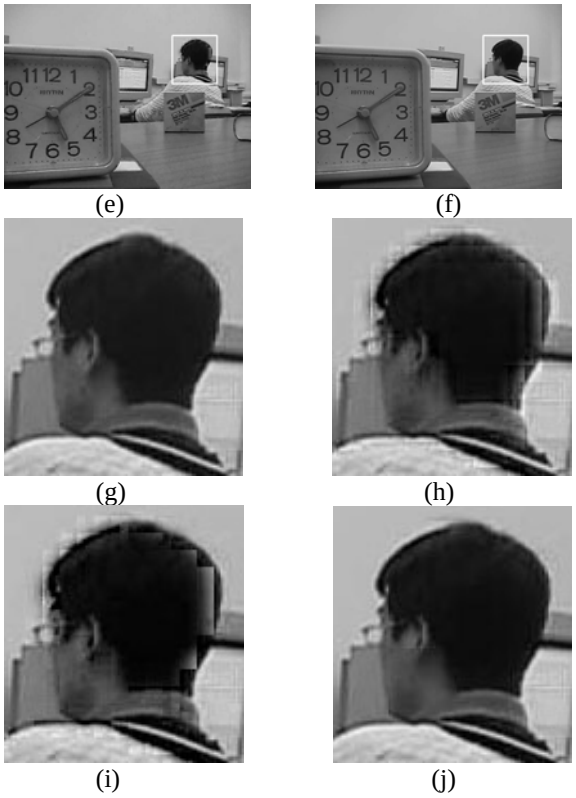

Fig. 4 The 'Lab' source images (size = 640 × 480) and fusion results: (a) reference image. (b) focus on the right. (c) focus on the left. (d) Haar wavelet result. (e) morphological wavelet result. (f) the result of the proposed algorithm. (g) - (j) are the local magnifications of (a), (d), (e) and (f), respectively.

1) RMSE measure

When there is a reference image, the RMSE measure is more suitable for performance evaluation. For reference image R and fused image F (both of size $I \times J$), the $RMSE$ is defined as follows.

$$RMSE = \sqrt{\frac{\sum_{i=1}^{I}\sum_{j=1}^{J}\left[R(i,j)-F(i,j)\right]^2}{I \times J}} \tag{5}$$

where $R(i,j)$ and $F(i,j)$ are the pixel values at position (i,j) of R and F, respectively. Smaller the value is, better is the fused performance. Table 2 shows the $RMSEs'$ of fused images in Figs. 3 - 4.

Table 2 RMSEs' of fused images

Figure	***Proposed Algorithm / Block size***	***Haar wavelet***	***Morphological wavelet [1]***
Fig. 3 (Disk)	3.8689 25×43	7.3015	7.8987
Fig. 4 (Lab)	2.3882 30×15	5.5665	5.9779

2) Similarity measure

Gradient or derivative operators are useful tools to measure the variation of intensity with respect to immediate neighboring points or pixels of an image. It is observed that a pixel possesses high gradient value when it is sharply focused. An objective criterion based on this knowledge is suggested to measure the quality of the results. Magnitude of gradient $G(r,c)$ at a point (r,c) of image X is obtained by

$$G(r,c) = \frac{1}{2}\{\left|X(r,c)-X(r+1,c+1)\right| + \left|X(r,c+1)-X(r+1,c)\right|\}. \tag{6}$$

$G(r,c)$ for the image with all parts properly focused may be obtained from various partially focused images as follows. For a set of n multi-focus images X_i, i = 1, . . . , n, the gradient images G_i, i = 1, . . . , n are obtained first. Then, G_i, i = 1, . . . , n are combined into G by taking the maximum gradient value at each position, i.e.

$$G(r,c) = \max\{G_1(r,c), G_2(r,c), ..., G_n(r,c)\} \quad \text{for all } (r,c) \tag{7}$$

Thus only the sharply focused regions from the constituent images have their contribution in the maximum gradient image G. Let G' denote the gradient image obtained from the reconstructed image X'. It is referred to as the gradient of fused image. Then, more similar G and G' are, better is the fusion algorithm. The similarity S between two images is calculated as follows:

$$S(G,G') = 1 - \frac{\sqrt{\sum (G(r,c)-G'(r,c))^2}}{\sqrt{\sum (G(r,c))^2} + \sqrt{\sum (G'(r,c))^2}} \tag{8}$$

Hence, for an ideal fused image S approaches the value 1. Similarity between maximum gradient and fused gradient images are list in Table 3.

Table 3 Similarity between maximum gradient and fused gradient images

Figure	***Proposed Algorithm / Block size***	***Haar wavelet***	***Morphological wavelet [1]***
Fig. 3 (Disk)	0.9122 25×43	0.8316	0.8152
Fig. 4 (Lab)	0.9204 30×15	0.8386	0.8430

Then we can get the conclusion from above that the results obtained by our method are superior to Haar wavelet

transform method and morphological wavelet method in both objective and visual evaluations.

6. Conclusion

In this paper we have presented a block based multi-focus image fusion algorithm using spatial frequency and GA, which combines pixel-level and feature-level fusion. The basic idea is to divide the source images into blocks, and then select the corresponding blocks with higher spatial frequency value to construct the resultant fused image. GA is brought forward to search for the optimized sizes of the block. Performance analysis reveals that our method outperforms the fusion by Haar wavelet and morphological wavelet method [1], particularly when there is movement in the objects or mis-registration of the source images.

References

[1] Ishita De, Bhabatosh Chanda: A simple and efficient algorithm for multifocus image fusion using morphological wavelets. Signal Processing 86 (2006) 924–936.

[2] W. Seales, S. Dutta, Everywhere-in-focus image fusion using controllable cameras, Proceedings of SPIE 2905, 1996, pp. 227–234.

[3] I. Bloch, Information combination operators for data fusion: a review with classification, IEEE Trans. SMC: Part A 26 (1996) 52–67.

[4] H.A. Eltoukhy, S. Kavusi, A computationally efficient algorithm for multi-focus image reconstruction, Proceedings of SPIE Electronic Imaging, June 2003.

[5] S. Mukhopadhyay, B. Chanda, Fusion of 2d gray scale images using multiscale morphology, Pattern Recognition 34 (2001) 1939–1949.

[6] P.J. Burt, R.J. Lolezynski, Enhanced image capture through fusion, in: Proceedings of the Fourth International Conference on Computer Vision, Berlin, Germany, 1993, pp. 173–182.

[7] H. Li, B. Manjunath, S. Mitra, Multisensor image fusion using the wavelet transform, Graph. Models Image Process. 57 (3) (1995) 235–245.

[8] X. Yang, W. Yang, J. Pei, Different focus points images fusion based on wavelet decomposition, Proceedings of Third International Conference on Information Fusion, vol. 1, 2000, pp. 3–8.

[9] Z. Zhang, R.S. Blum, Image fusion for a digital camera application, Conference Record of the Thirty-Second Asilomar Conference on Signals, Systems and Computers, vol. 1, 1998, pp. 603–607.

[10] Shutao Li, James T. Kwok, Yaonan Wang: Combination of images with diverse focuses using the spatial frequency. Information Fusion 2 (2001) 169–176.

[11] D.E. Goldberg, Genetic Algorithms in Search, Optimization and Machine Learning, Addison-Wesley, Reading, MA, 1992.

[12] Chin-Shiuh Shieha, Hsiang-Cheh Huangb, Feng-Hsing Wangc, Jeng-Shyang Pana, Genetic watermarking based on transform domain techniques, Pattern Recognition 37 (2004) 555 – 565.

Jun Kong was born in Jilin, China. He received the B.S and M.S degrees from the Department of Mathematics of Northeast Normal University, China, in 1992 and 1997, respectively. In 2001, he received the Ph.D. degree from College of Mathematics of Jilin University. From 2003 to 2004, he worked at Edith Cowan University, Perth, WA, Australia, as a visiting scholar. He is an associate professor and vice Dean of Computer School of Northeast Normal University. His research interests include artificial intelligence, digital image processing, pattern recognition, machine learning, biometrics and information security.

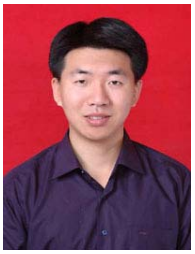

Kaiyuan Zheng was born in Jilin, China. He received his B.S degrees from Computer School of Northeast Normal University, China, in 2003. Now he is also pursuing his M.S degree in Computer School of Northeast Normal University. His main research interests are digital image processing, neural networks and pattern recognition.

Jingbo Zhang received her B.S and M.S degrees from Computer School of Northeast Normal University, China, in 1993 and 2004, respectively. Her main research interests are digital image processing, neural networks and pattern recognition.

Xue Feng was born in Jilin, China. She received her B.S degrees from Computer School of Northeast Normal University, China in 2005. Now she is also pursuing her M.S degree in Computer School of Northeast Normal University. Her main research interests are digital image processing, pattern recognition and information fusion.